Fish and Shellfish Immunology 93 (2019) 815–822

Contents lists available at ScienceDirect

Fish and Shellfish Immunology

journal homepage: www.elsevier.com/locate/fsi

Full length article

Identification of cells expressing two peptidoglycan recognition proteins in the gill of the vent mussel, *Bathymodiolus septemdierum*

Tetsuro Ikuta[a,*], Akihiro Tame[b], Masaki Saito[a], Yui Aoki[a], Yukiko Nagai[a], Makoto Sugimura[c], Koji Inoue[d], Katsunori Fujikura[a], Kazue Ohishi[a], Tadashi Maruyama[a], Takao Yoshida[a]

[a] Japan Agency for Marine-Earth Science and Technology (JAMSTEC), 2-15 Natsushima, Yokosuka, Kanagawa, 237-0061, Japan
[b] Marine Works Japan, Ltd., 3-54-1 Oppamahigashi, Yokosuka, Kanagawa, 237-0063, Japan
[c] Enoshima Aquarium, 2-19-1 Katasekaigan, Fujisawa, Kanagawa, 251-0035, Japan
[d] Department of Marine Bioscience, Atmosphere and Ocean Research Institute, The University of Tokyo, 5-1-5 Kashiwanoha, Kashiwa, Chiba, 277-8564, Japan

ARTICLE INFO

Keywords:
Immune response
Symbiont recognition
Peptidoglycan recognition protein
Bathymodiolus septemdierum
Chemosynthetic symbiosis
Horizontal symbiont transmission

ABSTRACT

In symbiotic systems in which symbionts are transmitted horizontally, hosts must accept symbionts from the environment while defending themselves against invading pathogenic microorganisms. How they distinguish pathogens from symbionts and how the latter evade host immune defences are not clearly understood. Recognition of foreign materials is one of the most critical steps in stimulating immune responses, and pattern recognition receptors (PRRs) play vital roles in this process. In this study, we focused on a group of highly conserved PRRs, peptidoglycan recognition proteins (PGRPs), in the deep-sea mussel, *Bathymodiolus septemdierum*, which harbours chemosynthetic bacteria in their gill epithelial cells. We isolated *B. septemdierum* PGRP genes *BsPGRP-S* and *BsPGRP-L*, which encode a short- and a long-type PGRP, respectively. The short-type PGRP has a signal peptide and was expressed in the asymbiotic goblet mucous cells in the gill epithelium, whereas the long-type PGRP was predicted to include a transmembrane domain and was expressed in gill bacteriocytes. Based on these findings, we hypothesize that the secreted and transmembrane PGRPs are engaged in host defence against pathogenic bacteria and/or in the regulation of symbiosis via different cellular localizations and mechanisms.

1. Introduction

Symbioses between bacteria and eukaryotes are found globally and have profound impacts on the ecology, physiology, and evolution of living organisms. In deep-sea hydrothermal vent and seep ecosystems, a wide variety of animals establish symbioses with chemosynthetic bacteria, which use the chemical energy of reduced sulphur, methane, or hydrogen from vent or seep fluid to produce organic carbon and provide their hosts with nutrition [1,2]. This metabolic dependence exerts a strong pressure on the stable transmission of symbionts to preserve the relationship. Symbiotic bacteria can be transmitted vertically (directly from parent to offspring, often via gametes), horizontally (between contemporary hosts or through reinfection by symbionts from a free-living population), or through a mixed-mode (a combination of the two above transmission mechanisms) [3]. Deep-sea mussels belonging to the genus *Bathymodiolus* dominate hydrothermal vents and methane seeps [1]. They harbour chemosynthetic bacteria in their gill epithelial cells, called bacteriocytes, as their primary nutritional source [4]. Their symbiotic bacteria are acquired horizontally from the environment [5]. Thus, while *Bathymodiolus* mussels accept symbionts in their gill epithelial cells, they must also recognize and reject exogenously invading microorganisms to maintain homeostasis. However, it remains unclear how they distinguish pathogens from symbionts, and how symbionts evade host immune defences.

Members of the peptidoglycan recognition protein (PGRP) family specifically bind to peptidoglycans (PGN), a major structural component of bacterial cell walls [6], and are believed to have evolved from bacteriophage T7 lysozyme, which can cleave PGN with its amidase activity [7]. Because eukaryotic cells do not contain PGN, it is an ideal target molecule for the detection of bacterial invasion. PGRPs are well-characterized in insects, particularly in the fruit fly (*D. melanogaster*). Based on protein structures, insect PGRPs have been divided into two classes: long PGRPs (PGRP-L), which have long transcripts encoding either intracellular or transmembrane proteins, and short PGRPs (PGRP-S), which are small extracellular proteins with an N-terminal signal peptide [8]. In general, transmembrane-PGRPs are involved in

* Corresponding author.
E-mail address: teikuta@jamstec.go.jp (T. Ikuta).

https://doi.org/10.1016/j.fsi.2019.08.022
Received 26 March 2019; Received in revised form 6 August 2019; Accepted 9 August 2019
Available online 13 August 2019

activation of the immune deficiency (Imd) signalling cascade or induction of phagocytosis by recognizing meso-diaminopimelic acid-containing (DAP-type) PGN from many Gram-negative and some Gram-positive bacteria. In contrast, secreted extracellular PGRPs activate melanisation or Toll signalling pathways, which produce antibacterial peptides primarily by recognizing L-lysine-type (Lys-type) PGN from Gram-positive bacteria [8,9].

PGRPs have been studied in some bivalve species and are thought to play a key role in immune response against pathogenic bacteria [10–13]. In *Bathymodiolus* mussels, PGRP genes have been identified from two species, *B. azoricus* and *B. platifrons* [14,15]. *B. azoricus* is a dominant member of the Mid-Atlantic Ridge (MAR) hydrothermal fauna in the Azores region that harbours two physiologically and phylogenetically distinct species of Gammaproteobacteria, sulphide and methane oxidizers [16]. In *B. azoricus*, five PGRPs have been identified (PGRP1-5); among these, two were predicted to be secreted, but none were predicted to be located at the membrane [14]. Based on the high correlation between loss of symbionts and decreased expression of PGRP paralogs in the gills of *B. azoricus*, the authors speculated that PGRPs might regulate symbiont acquisition [14]. The second species, *B. platifrons*, is common in hydrothermal vents and methane seeps in the Western Pacific Ocean, and harbours methane-oxidizing Gammaproteobacteria (Gram-negative) in its gill epithelium. In a previously reported transcriptome analysis, 11 transcripts were matched to PGRP sequences in *B. platifrons* and were grouped into three clusters. Based on amino acid sequence and gene expression analyses, the authors suggested that the *B. platifrons* PGRP isoforms have different cellular locations (intracellular or secretory, but not transmembrane), potentially distinct selectivity towards PGN, and differential expression in different organs (the gill, mantle, or foot) [15]. In addition, in the recent genome analysis of *B. platifrons*, twenty-three PGRP sequences were reported, some of which were likely recently tandemly duplicated [17], although their phylogenetic relationships with five *B. azoricus* PGRPs have been unknown. Thus, while the isoforms, structures, and expression patterns of *Bathymodiolus* PGRPs among organs or individuals (with or without symbionts) have been studied, their functional roles are still unknown. To assign more specific roles to *Bathymodiolus* PGRPs, the cells expressing these genes need to be identified.

B. septemdierum is a dominant species at hydrothermal vents in the Izu-Ogasawara Arc, Japan, and harbours a single ribotype of thioautotrophic Gammaproteobacteria in the gill [18,19]. In this study, we isolated two *B. septemdierum* PGRP genes; among their products, one was predicted to be secreted, and the other to be transmembrane. To compare expression levels of the two PGRPs among the organs (gill, foot, and mantle), we conducted quantitative PCR analysis. Furthermore, to identify the cells that transcribe them in the gill, we performed *in situ* hybridization (ISH) analysis and transmission electron microscopy (TEM). Based on these findings, we discuss the possible functions of two PGRPs in the gill of *B. septemdierum*.

2. Materials and methods

2.1. Screening for PGRP sequences in pyrosequencing data

Previously reported pyrosequenced RNA-seq data from the *B. septemdierum* gill [20] were screened by standalone TBLASTN analysis using amino acid sequences of PGRP proteins from *Mytilus galloprovincialis* [21], *B. platifrons* [15], and *B. azoricus* [14] as queries. The threshold of sequence homology was defined as an E-value ≤ 1.0e–5.

2.2. Phylogenetic and amino acid sequence analyses

To construct a phylogenetic tree, the amino acid sequences of PGRPs from several organisms were retrieved from the NCBI protein database and previous reports [14,15,17]. The conserved domain structure of the protein was analysed on the SMART server (http://smart.embl-heidelberg.de) [22]. Using the PGRP domain, the phylogenetic trees were constructed using the maximum-likelihood (ML) method in MEGA7 [23] with the WAG + G model of amino acid substitutions. Bootstrap values were obtained from 1000 resampling sequence alignments for the ML analysis. Signal peptides and transmembrane domains were predicted using the SignalP 4.1 (http://www.cbs.dtu.dk/services/SignalP/) [24] and TMHMM v.2.0 (http://www.cbs.dtu.dk/services/TMHMM/) [25] servers, respectively. The potential pathway for peptidoglycan biosynthesis in the *B. septemdierum* symbiont was estimated using data deposited in the KEGG database as reference [26], which was based on genome information for the *B. septemdierum* symbiont [19].

2.3. Animal sampling

B. septemdierum was collected from hydrothermal vent sites on the Myojin Knoll, at depths of 1278 m (Dive #1288), 1182 m (Dive #1810), and 1223 m (Dive #2056) during the cruises NT11-09 (15–26 June 2011), KY-15-07 (24–29 April 2015), and KS-18-3 (3–9 April 2018), respectively, with the ROV Hyper Dolphin operated by the R/V *Natsushima,* R/V *Kaiyo*, or R/V *Shinsei Maru* of the Japan Agency of Marine-Earth Science and Technology (JAMSTEC). Samples were also collected from hydrothermal vent site on the Suiyo Seamount at a depth of 1378 m (Dive #778) during cruise KR18-09 with the ROV Kaiko, operated by the R/V *Kairei* of JAMSTEC. The mussels were recovered alive, and the gills, feet, and mantles were immediately dissected onboard with disposable scalpels. For RNA extraction, the gills, feet, and mantles were placed into RNAlater (Qiagen, Hilden, Germany), incubated for 16 h at 4 °C, and stored at −80 °C. For DNA extraction, the gills were frozen in liquid nitrogen and stored at −80 °C. For *in situ* hybridization (ISH), the gills were fixed in 4% paraformaldehyde in 1 × PBS for 16 h at 4 °C, followed by stepwise dehydration in an ethanol series, and stored in 100% ethanol at −30 °C until use. For transmission electron microscopy (TEM), the gills were fixed at 4 °C in 2.5% glutaraldehyde in seawater filtered through a 0.22-μm filter (Nalgene, Rochester, NY, USA) (filtered seawater, FSW).

A fraction of the collected mussels was stored in shipboard aquarium tanks during the cruise. After the cruise, these mussels were immediately transported to the Enoshima Aquarium in Kanagawa, Japan, and reared in an aquarium tank with an average water temperature of 6.1 °C. After 62 days of rearing, three live mussels were dissected, and their gills were fixed for RNA extraction or frozen as described above.

2.4. Bacterial exposure experiment

Symbiotic bacteria were extracted from the gills of *B. septemdierum* as described previously [27]. The symbionts were fixed with 4% paraformaldehyde in FSW for 24 h at 4 °C, collected by centrifuging at 15,000 × *g* for 5 min at 4 °C, and washed with FSW. The fixed symbiont cells were incubated with 0.1% fluorescein isothiocyanate isomer I (FITC; Sigma-Aldrich, St. Louis, MO, USA) in 0.1 M sodium hydrogen carbonate (pH 9.0) and 10% dimethyl sulfoxide for 1 h at 4 °C. After the incubation, they were centrifuged at 15,000 × *g* for 5 min at 4 °C, washed six times with FSW, and used within a week for the exposure experiments.

For exposure experiments, the gills were excised on-board from three freshly collected mussels and cut into small pieces (3–5 mm width). The gill pieces were incubated with either Alexa Fluor 488 *Escherichia coli* BioParticles conjugates (Thermo Fisher Scientific, Waltham, MA, USA) or fixed symbionts prepared as above for 24 h at 4 °C in darkness (final density of 1×10^7 cells/mL in 9 mL FSW). For reference, the gill pieces were incubated in FSW for 24 h at 4 °C. After incubation, the gill pieces were rinsed with FSW, placed in RNAlater (Qiagen), incubated for 16 h at 4 °C, and stored at −80 °C.

2.5. RNA extraction and cDNA synthesis

For qPCR analysis, total RNA from the gills, feet, and mantles of three freshly collected mussels, the gills of three mussels reared in a tank for 62 days, and the gills from the bacterial exposure experiment was extracted using the classical guanidine thiocyanate method with pelleting through caesium chloride. The extracted RNA was treated with recombinant DNase I (Takara, Shiga, Japan) at 37 °C for 30 min, then purified using an RNAeasy Mini Kit (Qiagen). The cDNA was synthesized from 1 μg of total RNA using a PrimeScript II 1st strand cDNA Synthesis Kit (Takara) and oligo(dT) primers in a 20 μL reaction volume. After the reaction, UltraPure DNase/RNase-Free Distilled Water (UPDW, Thermo Fisher Scientific) was added to obtain a final volume of 100 μL. Reverse transcriptase was omitted (negative RT− control) for the negative control in the qPCR analysis. For the preparation of ISH probes, total RNA was extracted from the gill using an RNeasy Mini kit (Qiagen) with on-column DNase digestion according to the manufacturer's instructions. Synthesis of cDNA was performed as described above, and after the reaction UPDW was added to obtain a final volume of 200 μL.

2.6. Quantitative PCR (qPCR) for gene expression analysis

For quantitating PGRP mRNA, qPCR primers for the *BsPGRP-L*, *BsPGRP-S,* and *rL21* genes (ribosomal protein 21 for normalization, which was extracted from the RNA-seq data of the gill of *B. septemdierum* [20]) were designed using Primer Express software v.3.0 (Thermo Fisher Scientific). The qPCR primers used in this study are listed in Table S1. The sequences of the amplicons generated using these primers were confirmed by DNA sequencing. Triplicates of a 10-fold dilution series (from 10^{-5} to 10^{-9} pmol for *BsPGRP-L* and *rL21*, and from 10^{-6} to 10^{-10} pmol for *BsPGRP-S*) of the PCR fragment encompassing the region targeted by each qPCR primer set was used to produce calibration curves (*BsPGRP-L*: efficiency = 92.35%, slope = −3.520, *y*-intercept = 23.09, R^2 = 0.999; *BsPGRP-S*: efficiency = 91.99%, slope = −3.530, *y*-intercept = 24.13, R^2 = 0.999; *rL21*: efficiency = 95.25%, slope = −3.441, *y*-intercept = 24.69, R^2 = 0.999) for absolute quantification. The PCR primers used for template preparation to produce calibration curves are listed in Table S1. PCR was performed on an Applied Biosystems QuantStudio 3 Real-Time PCR System (Thermo Fisher Scientific) in 20-μL reaction mixtures containing 10 μL of Power SYBR Green PCR Master Mix (Thermo Fisher Scientific), 0.3 μM of each primer, and 1 μL of the cDNA template. The reaction conditions were 2 min at 50 °C, 2 min at 95 °C, 95 °C for 15 s and 60 °C for 1 min (40 cycles), and a ramped melting step from 60 °C to 95 °C to confirm the specificity of the amplified PCR products. For the bacterial exposure experiments, the relative abundance of PGRP transcripts was calculated using the $2^{-\Delta\Delta Cq}$ method [28]. All assays were performed in triplicate. No-template controls (NTC) containing 1 μL of H_2O instead of cDNA, as well as negative RT^- controls (see above), were included with every assay to ensure that genomic DNA did not contaminate the reactions. Quantification was performed using QuantStudio Design & Analysis Software v1.4.1 software (Thermo Fisher Scientific). Statistical analysis was performed using Microsoft Office Excel for Mac (Microsoft, Redmond, WA, USA), and *P* values were calculated using *t*-tests at the 5% significance level.

2.7. qPCR for symbiont abundance analysis

To analyse the abundance of the gill symbiont, total genomic DNA was extracted using the DNeasy Blood and Tissue Kit (Qiagen) from the gills of the mussels that were used for RNA extraction for qPCR. We used the primers previously described for quantification of the Bathymodiolin gill symbiont targeting the host 18S rRNA and the thiotrophic symbiont 16S rRNA [29] (Table S1). The qPCR conditions were as described previously, using 1 ng of DNA template and 0.5 μM of each primer [29]. Symbiont abundance was calculated using the $2^{-\Delta\Delta Cq}$ method [28], in which the threshold cycle (Cq) values of the symbiont 16S rRNA were normalized against the Cq values of the host 18S rRNA using data from the freshly collected mussels as a reference. The sequence of the PCR product amplified using the primers for thiotrophic symbiont 16S rRNA was confirmed by Sanger sequencing and was identical to the reported BSEPE (*B. septemdierum* endosymbiont) 16S rRNA sequence [19].

2.8. In situ hybridization (ISH)

PCR primer sets were designed to be specific for *BsPGRP-L*, *BsPGRP-S*, and the *16S rRNA* gene of the sulphur-oxidizing symbiont of *B. septemdierum* (Table S1). *BsPGRP-L* and *BsPGRP-S* were amplified from gill cDNA using the Easy-A High-Fidelity PCR Cloning Enzyme (Agilent Technologies, CA, USA). The *16S rRNA* gene was amplified from the genomic DNA extracted from the gill of *B. septemdierum*, as previously described [19]. The PCR fragments were cloned into pBluescript KS (Agilent Technologies), and the insert sequences were confirmed by DNA sequencing. Antisense riboprobes for *PGRP-L* and *-S* labelled with fluorescein and those for the symbiont 16S rRNA labelled with digoxigenin (DIG) were synthesized as previously described [30].

ISH of 4 μm transverse gill sections was performed as described previously [30,31], with the following modifications. Hybridization was performed in the presence of both DIG- and fluorescein-labelled probes at 60 °C overnight. After NBT/BCIP chromogenic staining to detect fluorescein labelled probes with 1:2000 anti-fluorescein-AP fab fragments (Sigma-Aldrich), sections were incubated with 1:2000 anti-digoxigenin-POD Fab fragments (Sigma-Aldrich) at 4 °C overnight, and signals were detected with 1:50 cyanine 3 plus amplification reagent in the amplification diluent buffer from the TSA Plus Cyanine 3/Fluorescein kit (PerkinElmer). For simultaneous detection of two-colour fluorescent signals, staining with tyramide signal amplification using the TSA Plus Cyanine 3/Fluorescein kit was conducted as previously described [30], and the first peroxidase enzyme was deactivated with 0.1 M glycine-HCl pH 2.0. All sections were mounted in Vectashield with or without DAPI (Vector Laboratories, CA, USA) and covered with a coverslip. Images were taken using an Olympus IX73 microscope (Olympus) equipped with an Olympus DP73 camera or a Nikon A1RMP confocal scanning system (Nikon, Tokyo, Japan). Micrographs were processed with Adobe Photoshop CS6 (Adobe Systems Inc., San Jose, CA, USA).

2.9. Transmission electron microscopy

Thin sections of the gill were prepared as previously described [32] with the following modifications. Gill pieces were post-fixed with 2.0% osmium tetroxide dissolved in filtered artificial seawater for 2 h at 4 °C. After washing with an aqueous solution of 8.0% sucrose, conductive staining was performed by incubation in 0.5% thiocarbohydrazide (Thermo Fisher Scientific) aqueous solution for 30 min and 1.0% osmium tetroxide aqueous solution for 1 h at 4 °C. Samples were dehydrated in a graded ethanol series and embedded in Epon 812 (TAAB, Aldermaston, UK). Ultrathin sections (60-nm) were cut with a diamond knife on an Ultracut S ultra-microtome (Leica Microsystems, Wetzlar, Germany), stained with 2.0% uranyl acetate and 2.0% lead citrate solutions, and observed using a Tecnai G2 20 transmission electron microscope (FEI, Hillsboro, OR, USA) at 120 kV.

3. Results

3.1. Identification of B. septemdierum PGRPs

From the RNA-seq database, two contigs (Bse_c00263 and Bse_c03545) encoding peptides with high similarity to *M. gallopro-vincialis* and *B. azoricus* PGRPs were obtained. Bse_c00263 consisted of

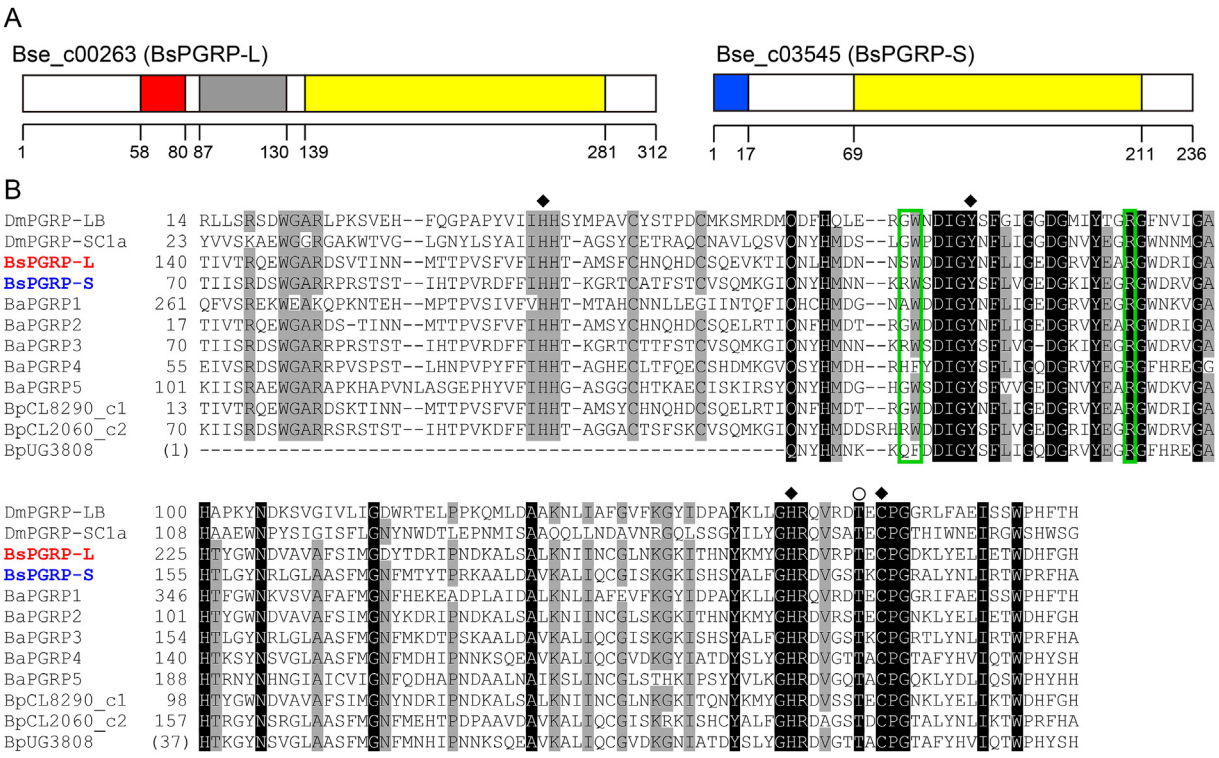

Fig. 1. Domain structures and amino acid sequence alignment of peptidoglycan recognition proteins (PGRPs) from *B. septemdierum*. (A) Domain structures of the products of Bse_c00263 (*BsPGRP-L*) and Bse_c03545 (*BsPGRP-S*). Yellow and grey boxes indicate the putative PGRP/amidase domain and WAP domain, respectively. Red and blue boxes indicate the transmembrane domain and the N-terminal signal peptide, respectively. (B) Amino acid sequence alignment of PGRP domains from multiple *Bathymodiolus* spp. Black and grey shadings indicate positions at which amino acid residues are conserved or highly similar, respectively. Green boxes enclose residues implicated in peptidoglycan selectivity. ◆: Zn^{2+}-binding sites for amidase activity, ○: threonine residues involved in catalytic activity or recognition of PGN. DmPGRP-LB and DmPGRP-SC1a: *D. melanogaster* PGRP LB (NP_001247052 in GenBank) and PGRP SC1a (NP_610407 in GenBank), respectively. BaPGRP1-5: *B. azoricus* PGRP 1–5 [14]. BpCL8290_c1, BpCL2060_c2, BpUG3808: *B. platifrons* PGRPs CL8290_contig1, CL2060_contig2, and Unigene3808, respectively [15]. Only a 3′ partial sequence has been reported for BpUG3808. (For interpretation of the references to colour in this figure legend, the reader is referred to the Web version of this article.)

1,828 nts, and the ATG at nucleotide positions 57–59 was assigned as the translational initiation codon for a complete open reading frame (ORF) of 939 bps, encoding 312 amino acid residues. SMART analysis showed that the product of Bse_c00263 has a transmembrane domain, a whey acidic protein (WAP) domain [33], and a PGRP domain (E-value, 1.64e-64) (Fig. 1A). Bse_c03545 consisted of 836 nts, and the ATG at nucleotide positions 69–71 was assigned as the translational initiation codon. Based on this, Bse_c03545 has a complete open reading frame (ORF) of 711 bps encoding 236 amino acid residues. SMART analysis showed that the product of Bse_c03545 has a PGRP domain (E-value, 1.76e-64) (Fig. 1A). SignalP analysis indicated that the first 17 amino acid residues constitute a signal peptide (Fig. 1A).

In a phylogenetic analysis with maximum likelihood, the product of Bse_c00263 was placed in a clade with *B. azoricus* PGRP2 and *B. platifrons* CL8290 (bootstrap value of 95%, Fig. 2), while the product of Bse_c03545 was placed in a clade with *B. azoricus* PGRP3, *B. platifrons* CL2060, and *M. gallopro*vincialis PGRP3 (bootstrap value of 98%, Fig. 2). Based on these results, we designated Bse_c00263 and Bse_c03545 as *BsPGRP-L* (*B. septemdierum* PGRP-long type) and *BsPGRP-S* (*B. septemdierum* PGRP-short type), respectively. cDNA sequences of *BsPGRP-L* and *BsPGRP-S* were submitted to DDBJ under accession numbers LC467148 and LC467149, respectively. In our additional phylogenetic analysis, all available *Bathymodiolus* PGRP sequences (including the high number of PGRPs from *B. platifrons* transcriptome and genome analysis) were grouped into five clusters (Fig. S1).

3.2. Amino acid sequence analysis of B. septemdierum PGRPs

Domain searches on the SMART server detected PGRP domains in both PGRPs of *B. septemdierum* with significant values. The amino acid sequence alignment shows that four Zn^{2+}-binding sites (His42, Tyr78, His152, and Cys160 in DmPGRP-LB) for amidase activity and a threonine residue (Thr158 in DmPGRP-LB) involved in catalytic activity or recognition of PGN [34] were completely conserved in both BsPGRP-L and -S (Fig. 1B). It has been reported that three amino acid residues (Gly80, Trp81, and Arg100 in DmPGRP-SC1a) are involved in binding selectivity for DAP-type PGN [35,36] (Fig. 1B). In BsPGRP-L and -S, the tryptophan and arginine residues are conserved, but the first residue is variable (serine in BsPGRP-L and arginine in BsPGRP-S) (Fig. 1B).

3.3. Expression pattern of B. septemdierum PGRPs

The expression levels of the two BsPGRPs in the gill, foot, and mantle of the freshly collected mussels were investigated by qPCR. Transcription of *BsPGRP-L* and *-S* was detected in all three organs, and expression levels of both genes in the gill were considerably higher than those in the foot and mantle (Fig. 3A). Thus, the gill is the principal organ in which the two BsPGRPs are expressed. In addition, the expression of these genes was analysed in the gills of the mussels reared in an aquarium for 62 days. The transcription levels of both genes were significantly lower in the reared mussels, in which the gill symbiont was not detected (Fig. 3A and B). Moreover, the relative expression levels of the two BsPGRPs in the gills exposed to fixed *E. coli* or symbiotic bacteria were analysed. The transcription level of *BsPGRP-L* in the gills exposed to fixed *E. coli* and that exposed to the fixed symbiont were

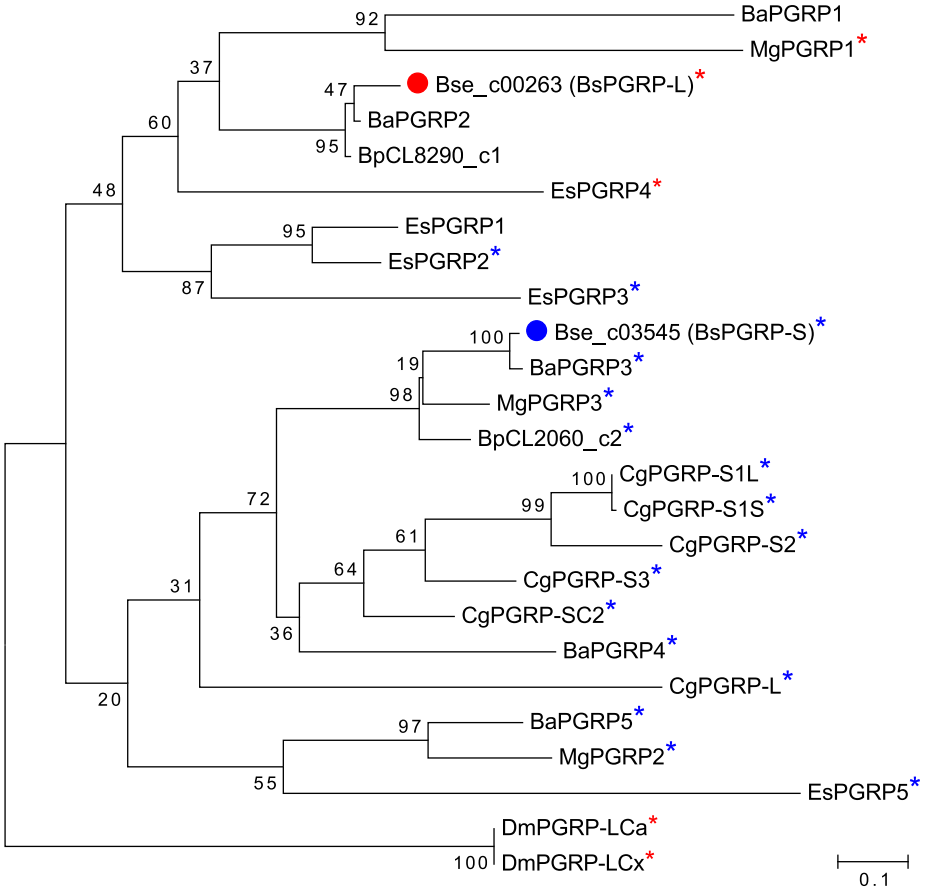

Fig. 2. Maximum-likelihood tree constructed from PGRP domain sequences from *Bathymodiolus* mussels and other molluscs. BsPGRP-L and -S are marked by red and blue dots, respectively. Bootstrap values (1000 replicates) are shown at the branches. The scale bar indicates 0.1 amino acid substitutions per position in the sequence. PGRPs with N-terminal signal peptides are marked with blue asterisks. PGRPs with transmembrane domains are marked with red asterisks. Abbreviations: Ba, *Bathymodiolus azoricus*; Bs, *Bathymodiolus septemdierum*; Bp, *Bathymodiolus platifrons*; Cg, *Crassostrea gigas*, Dm, *Drosophila melanogaster*; Es, *Euprymna scolopes*, Mg, *Mytilus galloprovincialis*. BaPGRP1-5: *B. azoricus* PGRP 1–5 [14]. BpCL8290_c1 and BpCL2060_c2: *B. platifrons* PGRPs CL8290_contig1 and CL2060_contig2, respectively [15]. Unigene3808 from *B. platifrons* (BpUG3808) was not included in this analysis as only partial sequence is available. GenBank accession numbers: NP 001295767 (CgPGRP-S1L), BAG31896 (CgPGRP-S1S), BAG31898 (CgPGRP-S2), BAG31899 (CgPGRP-S3), EKC26200 (CgPGRP-SC2), NP 001295777 (CgPGRP-L), AAY27973 (EsPGRP1), AAY27974 (EsPGRP2), AAY27975 (EsPGRP3), AAY27976 (EsPGRP4), AIR71819 (EsPGRP5), AJQ21530 (MgPGRP1), AJQ21531 (MgPGRP2), AJQ21541 (MgPGRP3), AAF50302.3 (DmPGRP-LCa), AAM18530.1 (DmPGRP-LCx). (For interpretation of the references to colour in this figure legend, the reader is referred to the Web version of this article.)

significantly higher than that of the reference samples. On the contrary, the gill expression level of *BsPGRP-S* after exposure to either bacteria was not significantly different from that of the reference samples (Fig. 3C).

To identify the gill cells expressing *BsPGRP-L* and *-S* in *B. septemdierum*, we performed ISH. The 16S rRNA signal from the endosymbionts was detected in the apical side of epithelial cells in the inner area of the gill filament, which is consistent with previous observations (Fig. 4C and F) [18,19]. The *BsPGRP-L* signal was detected throughout the cell cytoplasm, in the apical part of which the endosymbionts were localized (Fig. 4A–C). Thus, we conclude that *BsPGRP-L* is expressed in bacteriocytes. The *BsPGRP-S* signal was detected in goblet-shaped cells sparsely distributed in the abfrontal area of the gill (Fig. 4D–F). In confocal micrographs of fluorescent two-colour ISH, the *BsPGRP-S* signal did not overlap with the *16S rRNA* signal of the symbiont (Fig. 4G), indicating that *BsPGRP-S* is expressed in cells in which the symbiont has not colonized. In these sections, some droplet-like structures were observed in the cells with *BsPGRP-S* signal (arrowheads in Fig. 4G). Furthermore, through TEM analysis, dense globules of mucus were observed in the goblet-shaped cells of the abfrontal area (Fig. 4H). It has been shown that the abfrontal edge of the *Bathymodiolus* gill is abundantly populated by asymbiotic goblet mucous cells [37]. These observations indicate that *BsPGRP-S* is expressed in the asymbiotic goblet mucous cells at the abfrontal area of the gill filament.

4. Discussion

In this study, we isolated two new PGRPs from *B. septemdierum*. From phylogenetic and amino acid sequence analyses, they were

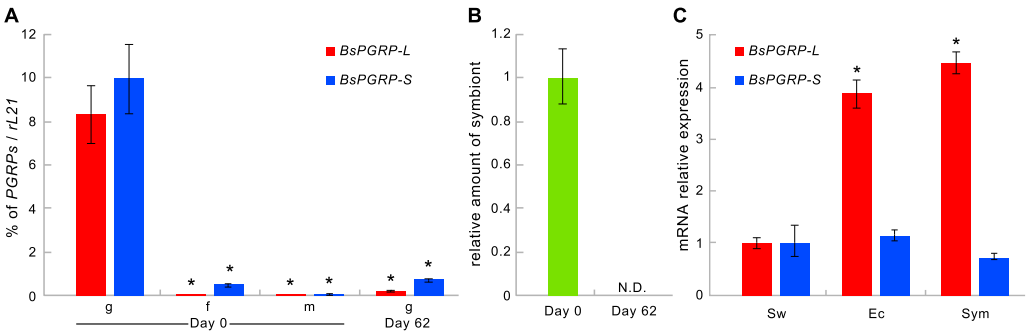

Fig. 3. Expression levels of *B. septemdierum* PGRPs. (A) Transcript levels of *BsPGRP-L* and *BsPGRP-S* mRNA analysed by qPCR in the gill (g), foot (f) and mantle (m) of freshly collected mussels and mussels reared in an aquarium for 62 days. Amounts of mRNA from the target genes normalized by the amount of *rL21* gene are given as means ± standard deviations. Asterisks indicate statistically significant differences relative to the gill of freshly collected mussels. (B) Relative amounts of symbiont in the gills of the mussels reared in an aquarium for 62 days compared to those observed in the freshly collected mussels. Error bar indicates the error range ($2^{-(\Delta\Delta Cq \pm s)}$, s = standard deviation). N.D., not detected. (C) Relative transcription levels of *BsPGRP-L* and *-S* in the gills exposed to fixed *E. coli* (Ec) or symbiotic bacteria (Sym). Sw: reference (gills incubated in FSW). Error bars indicate the error range ($2^{-(\Delta\Delta Cq \pm s)}$). Asterisks indicate statistically significant differences relative to reference samples.

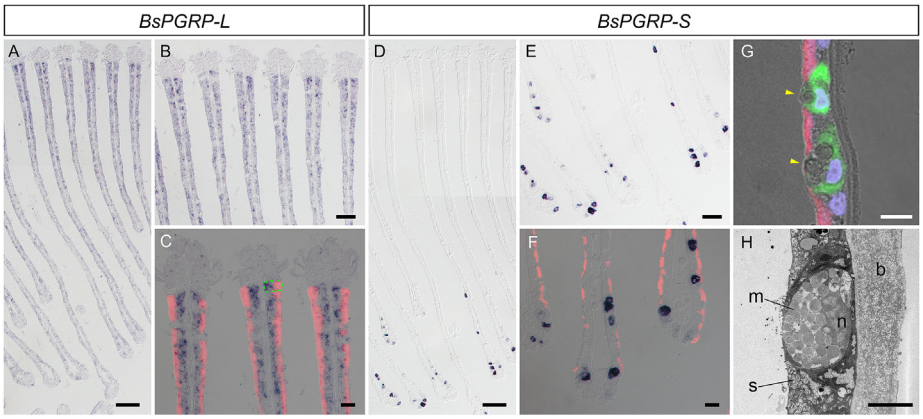

Fig. 4. Identification of cells expressing *BsPGRP-L* and *BsPGRP-S* in the gill. (A–G) ISH images of the gill. Frontal is at the top. (A, D) Two images stitched manually to show expression of BsPGRPs through the transverse section of the gill filaments. (B, E) Magnification of the frontal and abfrontal area, respectively. (C, F) Higher magnification with red fluorescence signals for the 16S rRNA of the symbiont. A single bacteriocyte is outlined with a green dotted line in C. (G) Fluorescent ISH signals (green for *BsPGRP-S* and red for the symbiont) were merged with DAPI signals and DIC images, all of which were obtained using confocal microscopy. Yellow arrowheads indicate droplet-like structures in the cells expressing *BsPGRP-S*. (H) TEM image showing a goblet-shaped cell with dense globules of mucus (m) in the gill epithelium; b, basal membrane; n, nucleus; s, symbiont. Scale bars in (A, D) 100 μm; (B, E) 50 μm; (C, F) 20 μm; (G) 10 μm; (H) 5 μm. (For interpretation of the references to colour in this figure legend, the reader is referred to the Web version of this article.)

assigned as long-type *BsPGRP-L* and short-type *BsPGRP-S* (Figs. 1 and 2). We also found that the gill, in which the symbiont is harboured, is the principal organ where both PGRPs are expressed (Fig. 3). It has been reported that in *B. platifrons*, CL8290, predicted to be orthologous to BsPGRP-L, is highly transcribed in the gill, whereas CL2060, predicted to be orthologous to BsPGRP-S, is highly transcribed in the gill and mantle [15]. In *B. azoricus*, PGRP2 and PGRP3, which are orthologous to BsPGRP-L and -S, respectively, have been reported to be expressed in the gill, although the expression level of PGRP2 is very low [14].

Our ISH and TEM experiments revealed that BsPGRP-S with a signal peptide is expressed in the asymbiotic goblet mucous cells at the abfrontal area of the gill filament. Based on the general morphology of animal epithelial cells [38], the localization of the nucleus (basal) and mucus globules (apical) in the cell indicate that mucus is secreted from the apical side of the cell to the outside of the gill. Mammalian PGRP-S is secreted from M cells located in the gut epithelial mucosa, where it plays a critical role in gut mucosal immunity [39]. In bivalves, seawater is drawn into the body through the gills, where tiny particles, including bacteria in the water, are caught in the gill mucus. Therefore, the bivalve gill is the leading edge of exposure to external pathogenic and symbiotic bacteria. Our amino acid sequence analysis of BsPGRP-S showed that it possesses an N-terminal signal peptide, the four Zn^{2+}-binding sites required for amidase activity, and the threonine residue involved in catalytic activity or recognition of PGN [34]. In addition, the glycine residue (Gly80 in DmPGRP SC1a), one of the amino acid residues responsible for selective PGRP binding to DAP-type PGN [35,36], which the *B. septemdierum* symbiont can produce [19], is replaced by an arginine residue in BsPGRP-S. The same substitution has been observed in other *Bathymodiolus* orthologues, namely *B. azoricus* PGRP3 and *B. platifrons* CL2060 (Fig. 1B) [14,15]. The amino acid residue of this position in *Mytilus* PGRP3, predicted to be orthologous to *BsPGRP-S* in our phylogenetic tree, is replaced by an histidine residue, unlike in these *Bathymodiolus* mussels [21]. Although the effect of this substitution on PGRP binding specificity is unknown, it suggests that BsPGRP-S may recognize DAP-type PGN with lower affinity, or the other type of PGN. *Mytilus PGRP3* has been shown to be expressed in the gill, and upregulated at 12 and 24 h post-exposure to various *Vibrio* strains [13], suggesting that *Mytilus* PGRP3 plays a role in host defence against pathogenic bacteria. However, our qPCR data showed that the expression level of *BsPGRP-S* was not significantly affected by gill exposure to either the fixed *E. coli* or symbiont (Fig. 3C). It has been reported that *B. azoricus PGRP3* was upregulated after a 24 h exposure to seawater, while little effect was observed with various *Vibrio* strains and *Flavobacterium* [13,40]. Thus, we hypothesize that BsPGRP-S produced in the asymbiotic goblet mucous cells is secreted into the mucus surrounding the gill, where it can contribute to the mucosal immune response against pathogenic bacteria, but not against the bacteria tested in these studies (*Vibrio*, *Flavobacterium*, and symbiotic bacterium).

In *Drosophila*, two PGRPs (SC1 and SC2) with amidase activity are expressed in the gut and are assumed to cleave the PGN of pathogenic bacteria, attenuating the immune response in the *Drosophila* gut [41]. Considering that such modulation of host immune activity is also a major function of PGRPs in interactions between animals and symbiotic bacteria [42], it is possible that BsPGRP-S is involved in symbiosis via attenuation of the host immune response in the gill. Notably, in the squid *Euprymna scolopes*, EsPGRP2, with amidase activity and potentially high binding affinity for Gram-negative PGN, is secreted into the lumen of the juvenile light organ, extracellularly colonized by the luminous Gram-negative bacterial symbiont, *Vibrio fischeri*. The authors suggested that EsPGRP2 plays a general role in host defence as well as a more specific role in regulating symbiosis by neutralizing the tracheal cytotoxin (TCT), a monomeric fragment of PGN from Gram-negative symbiotic bacteria [43]. However, if BsPGRP-S is engaged in the attenuation of the host immune response to regulate symbiosis, it is difficult to explain why its expression was not upregulated upon exposure to the symbiont. To more precisely understand the roles of BsPGRP-S, further functional studies are required. Our qPCR analysis showed that the expression level of *BsPGRP-S*, similar to that of its orthologue, *B. azoricus PGRP3* [14], was reduced in the reared individuals, which had fewer symbionts. This may be due to a change in the microbial environment from the habitat to the aquarium that affected the host immune response. Moreover, the loss of symbionts might lead to a reduction of energy supply needed for host defence against pathogens, which may result in decreased expression of *BsPGRP-S*, as has been suggested previously for *B. azoricus* PGRPs [14].

With regard to BsPGRP-L, our amino acid sequence analysis showed that it possesses a transmembrane domain, four Zn^{2+}-binding sites required for amidase activity, and a threonine residue involved in catalytic activity or recognition of PGN [34]. Additionally, the glycine residue (Gly80 in DmPGRP SC1a), one of the amino acid residues responsible for selective PGRP binding to DAP-type PGN [35,36], is replaced by a serine in BsPGRP-L. In our phylogenetic tree, BsPGRP-L was in a clade with *B. azoricus* PGRP2 and *B. platifrons* CL8290 (Fig. 2). However, this substitution was not observed in the two orthologues (Fig. 1B) [14,15]. In the cereal weevil *Sitophilus zeamais*, PGRP-LB, which has the same substitution, displays strong specificity toward TCT [44], suggesting that BsPGRP-L also may have an affinity for TCT derived from DAP-type PGN. Furthermore, the transmembrane domain has not been found in BaPGRP2 and CL8290, and transmembrane PGRPs have never been reported for *Bathymodiolus* mussel. Therefore, this is the first report describing a transmembrane-PGRP for this group. In the squid *E. scolopes*, the transmembrane-PGRP (EsPGRP4) is expressed in the juvenile light organ [45]; however, its function has not

been explored. Our ISH analysis revealed that *BsPGRP-L* is expressed in bacteriocytes within the gill filament. However, the subcellular localization of BsPGRP-L is currently unknown. The lumen of the mussel gill filament is filled with haemolymph, and the basal side of the bacteriocyte faces the haemolymph via the thick basal membrane [37]. Haemolymph is a critical player in invertebrate immunity associated with PGRPs [46]. However, because the inside of the gill lumen is delimited by a thick basal membrane (Fig. 4), it is unlikely that BsPGRP-L on the basal surface of the bacteriocyte can effectively recognize bacteria that invade into the haemolymph. Instead, BsPGRP-L is more likely localized on the apical membrane of the bacteriocyte, where it recognizes PGN of bacteria (or TCT derived from it) in the extracellular milieu. In *Drosophila*, membrane-bound PGRP-LC on the apical side of the gut epithelium has been reported to be involved in controlling immune response via the Imd pathway by recognizing DAP-type PGN of Gram-negative bacteria [47]. Because the key Imd adaptor molecule is lacking and no functionally homologous component has been identified yet in bivalves, it is unknown whether the Imd pathway exists and is involved in the response to Gram-negative bacteria in bivalves [48]. Thus, further investigations are necessary to confirm the role of BsPGRP-L in triggering an immune cascade. Concomitantly, the relationship between Imd pathway regulation and symbiosis has been shown in insects [49], but remains unknown in *Bathymodiolus* mussels.

Nonetheless, the specific expression of *BsPGRP-L* in the gill bacteriocytes presumes a potential function linked to endosymbiosis. In *Drosophila*, PGRP-LC has been suggested to play a role in phagocytosis of Gram-negative bacteria; however, it is unknown whether it functions directly as a phagocytic receptor [50]. TEM observations of the discontinuous cell membrane at the apical surfaces of bacteriocytes of *Bathymodiolus* mussels suggest that their symbionts are acquired from the environment by phagocytosis at the apical side of the bacteriocyte [5,51]. These observations raise the possibility that membrane-bound BsPGRP-L is involved in symbiosis at the apical membrane of bacteriocytes by regulation of phagocytosis, thereby regulating symbiont acquisition. A recent genomic study in *B. platifrons* proposed a molecular model for the phagocytic process in symbiont acquisition [17]. However, cellular expressions and functions of the relevant molecules have never been investigated. Classically, phagocytosis is thought to be involved in the acquisition of intracellular symbionts from the origin of eukaryotes to the present symbiotic systems [52–54]. Although the cellular and molecular mechanisms of symbiont acquisition via phagocytic events have been relatively well-studied in cnidarian-algal symbiosis [55], this information is poorly available in other organisms. Future studies focusing on these aspects in a wide variety of organisms, including *Bathymodiolus* symbiosis, would provide clearer overview of symbiosis. Our qPCR analysis showed that the expression of *BsPGRP-L* was up-regulated upon gill exposure to either the fixed *E. coli* or symbiotic bacteria (Fig. 3C). This suggests that BsPGRP-L localized on the apical membrane of the bacteriocyte may recognize these bacteria in the extracellular milieu and is positively regulated by their presence. If BsPGRP-L is involved in the acquisition of symbionts, symbiotic bacteria and other bacteria with PGN to which BsPGRP-L can bind may not be strictly distinguished upon initial recognition by the host.

As discussed above for *BsPGRP-S*, decreased expression of *BsPGRP-L* in the reared mussels (Fig. 3) might be caused by a change in the microbial environment surrounding the gill or a reduction of energy supply for defence. Colonization of *B. azoricus* symbiont in the newly formed gill epithelium has been studied in detail, but it is unknown how symbiont abundance increases during gill growth and whether symbionts are continuously acquired at the apical ends of bacteriocytes throughout the gill [56]. However, reacquisition of symbionts in the gills of reared and starved *B. azoricus* individuals from the freshly collected mussels has been observed [57], suggesting that all bacteriocytes in the gill can acquire the symbiont. If this is also the case for *B. septemdierum* and if BsPGRP-L is involved in symbiont acquisition, BsPGRP-L should be expressed at least at low levels in the reared individuals, as observed by our qPCR analysis. At this moment, however, we do not exclude the possibility that BsPGRP-L is involved in host defence against pathogenic bacteria.

In conclusion, we suggest that BsPGRP-S produced in the asymbiotic goblet mucous cells of the gill is secreted extracellularly into the gill mucus, and BsPGRP-L expressed in bacteriocytes in the gill is localized to the apical membrane of the bacteriocyte. Via different cellular localizations and mechanisms, each PGRP may be engaged in host defence against pathogenic bacteria and/or the regulation of symbiosis. However, further functional studies are required to better understand their roles. From three *Bathymodiolus* species, different numbers of PGRPs have been identified (twenty-three in five clusters in *B. platifrons* [15,17], five in *B. azoricus* [14], and two in *B. septemdierum*), though it is possible that the current lists of PGRPs are incomplete. Moreover, we have isolated a transmembrane PGRP (BsPGRP-L) for the first time in *Bathymodiolus* mussels, and one of the amino acid residues critical to DAP-type PGN binding was not found to be conserved. In addition, expression levels of BsPGRP-L orthologs in the gill seem to vary (high in *B. septemdierum* and *B. platifrons* [15], but very low in *B. azoricus* [14]). These differences might reflect differences in the type of chemosynthetic symbiosis—i.e., *B. platifrons* with methanotrophic bacteria, *B. septemdierum* with thiotrophic bacteria, and dual symbiosis in *B. azoricus* with both methanotrophic and thiotrophic bacteria. Each mussel species may have independently evolved some PGRP functions according to differences in symbiosis.

Acknowledgments

We are grateful to Dr. Yuki Hongo from the Japan Fisheries Research and Education Agency and Dr. Yue Him Wong from the Akita Prefectural University for their support with sequence data collection. We thank Dr. Motohiro Shimanaga from Kumamoto University, Dr. Tomoko Koito from Nihon University, Dr. Shojiro Ishibashi from JAMSTEC, and Dr. Takashi Toyofuku from JAMSTEC as well as the captains and crew of the R/V *Natsushima*, R/V *Kaiyo*, R/V *Shinsei Maru*, R/V *Kaiko*, the ROV Hyper Dolphin, and the ROV Kairei for helping with sample collection.

Appendix A. Supplementary data

Supplementary data to this article can be found online at https://doi.org/10.1016/j.fsi.2019.08.022.

References

[1] N. Dubilier, C. Bergin, C. Lott, Symbiotic diversity in marine animals: the art of harnessing chemosynthesis, Nat. Rev. Microbiol. 6 (10) (2008) 725–740.
[2] J.M. Petersen, F.U. Zielinski, T. Pape, R. Seifert, C. Moraru, R. Amann, S. Hourdez, P.R. Girguis, S.D. Wankel, V. Barbe, E. Pelletier, D. Fink, C. Borowski, W. Bach, N. Dubilier, Hydrogen is an energy source for hydrothermal vent symbioses, Nature 476 (7359) (2011) 176–180.
[3] M. Bright, S. Bulgheresi, A complex journey: transmission of microbial symbionts, Nat. Rev. Microbiol. 8 (3) (2010) 218–230.
[4] C.R. Fisher, Chemoautotrophic and methanotrophic symbioses in marine invertebrates, Rev. Aquat. Sci. 2 (1990) 399–436.
[5] Y.J. Won, S.J. Hallam, G.D. O'Mullan, I.L. Pan, K.R. Buck, R.C. Vrijenhoek, Environmental acquisition of thiotrophic endosymbionts by deep-sea mussels of the genus *Bathymodiolus*, Appl. Environ. Microbiol. 69 (11) (2003) 6785–6792.
[6] R.J. Guan, R.A. Mariuzza, Peptidoglycan recognition proteins of the innate immune system, Trends Microbiol. 15 (3) (2007) 127–134.
[7] A.M. Montano, F. Tsujino, N. Takahata, Y. Satta, Evolutionary origin of peptidoglycan recognition proteins in vertebrate innate immune system, BMC Evol. Biol. 11 (2011) 79.
[8] R. Dziarski, Peptidoglycan recognition proteins (PGRPs), Mol. Immunol. 40 (12) (2004) 877–886.
[9] J.A. Hoffmann, The immune response of Drosophila, Nature 426 (6962) (2003) 33–38.
[10] N. Itoh, K.G. Takahashi, Distribution of multiple peptidoglycan recognition proteins in the tissues of Pacific oyster, *Crassostrea gigas*, Comp. Biochem. Physiol. B Biochem. Mol. Biol. 150 (4) (2008) 409–417.
[11] D.J. Ni, L.S. Song, L.T. Wu, Y.Q. Chang, Y.D. Yu, L.M. Qiu, L.L. Wang, Molecular cloning and mRNA expression of peptidoglycan recognition protein (PGRP) gene in

bay scallop (*Argopecten irradians*, Lamarck 1819), Dev. Comp. Immunol. 31 (6) (2007) 548–558.
[12] X.M. Wei, J.M. Yang, D.L. Yang, J. Xu, X.Q. Liu, J.L. Yang, J.H. Fang, H.J. Qiao, Molecular cloning and mRNA expression of two peptidoglycan recognition protein (PGRP) genes from mollusk *Solen grandis*, Fish Shellfish Immunol. 32 (1) (2012) 178–185.
[13] E. Martins, A. Figueras, B. Novoa, R.S. Santos, R. Moreira, R. Bettencourt, Comparative study of immune responses in the deep-sea hydrothermal vent mussel *Bathymodiolus azoricus* and the shallow-water mussel *Mytilus galloprovincialis* challenged with *Vibrio* bacteria, Fish Shellfish Immunol. 40 (2) (2014) 485–499.
[14] C. Detree, F.H. Lallier, A. Tanguy, J. Mary, Identification and gene expression of multiple peptidoglycan recognition proteins (PGRPs) in the deep-sea mussel *Bathymodiolus azoricus*, involvement in symbiosis? Comp. Biochem. Physiol. B Biochem. Mol. Biol. 207 (2017) 1–8.
[15] Y.H. Wong, J. Sun, L.S. He, L.G. Chen, J.W. Qiu, P.Y. Qian, High-throughput transcriptome sequencing of the cold seep mussel *Bathymodiolus platifrons*, Sci. Rep. 5 (2015) 16597.
[16] S. Duperron, T. Nadalig, J.C. Caprais, M. Sibuet, A. Fiala-Medioni, R. Amann, N. Dubilier, Dual symbiosis in a Bathymodiolus sp. mussel from a methane seep on the Gabon continental margin (Southeast Atlantic): 16S rRNA phylogeny and distribution of the symbionts in gills, Appl. Environ. Microbiol. 71 (4) (2005) 1694–1700.
[17] J. Sun, Y. Zhang, T. Xu, Y. Zhang, H. Mu, Y. Zhang, Y. Lan, C.J. Fields, J.H.L. Hui, W. Zhang, R. Li, W. Nong, F.K.M. Cheung, J.W. Qiu, P.Y. Qian, Adaptation to deep-sea chemosynthetic environments as revealed by mussel genomes, Nat. Ecol. Evol. 1 (5) (2017) 121.
[18] Y. Fujiwara, K. Takai, K. Uematsu, S. Tsuchida, J.C. Hunt, J. Hashimoto, Phylogenetic characterization of endosymbionts in three hydrothermal vent mussels: influence on host distributions, Mar. Ecol. Prog. Ser. 208 (2000) 147–155.
[19] T. Ikuta, Y. Takaki, Y. Nagai, S. Shimamura, M. Tsuda, S. Kawagucci, Y. Aoki, K. Inoue, M. Teruya, K. Satou, K. Teruya, M. Shimoji, H. Tamotsu, T. Hirano, T. Maruyama, T. Yoshida, Heterogeneous composition of key metabolic gene clusters in a vent mussel symbiont population, ISME J. 10 (4) (2016) 990–1001.
[20] T. Nagasaki, Y. Hongo, T. Koito, I. Nakamura-Kusakabe, S. Shimamura, Y. Takaki, T. Yoshida, T. Maruyama, K. Inoue, Cysteine dioxygenase and cysteine sulfinate decarboxylase genes of the deep-sea mussel *Bathymodiolus septemdierum*: possible involvement in hypotaurine synthesis and adaptation to hydrogen sulfide, Amino Acids 47 (3) (2015) 571–578.
[21] M. Gerdol, P. Venier, An updated molecular basis for mussel immunity, Fish Shellfish Immunol. 46 (1) (2015) 17–38.
[22] I. Letunic, P. Bork, 20 years of the SMART protein domain annotation resource, Nucleic Acids Res. 46 (D1) (2018) D493–D496.
[23] S. Kumar, G. Stecher, K. Tamura, MEGA7: molecular evolutionary genetics analysis version 7.0 for bigger datasets, Mol. Biol. Evol. 33 (7) (2016) 1870–1874.
[24] T.N. Petersen, S. Brunak, G. von Heijne, H. Nielsen, SignalP 4.0: discriminating signal peptides from transmembrane regions, Nat. Methods 8 (10) (2011) 785–786.
[25] A. Krogh, B. Larsson, G. von Heijne, E.L.L. Sonnhammer, Predicting transmembrane protein topology with a hidden Markov model: application to complete genomes, J. Mol. Biol. 305 (3) (2001) 567–580.
[26] H. Ogata, S. Goto, K. Sato, W. Fujibuchi, H. Bono, M. Kanehisa, KEGG: Kyoto Encyclopedia of genes and genomes, Nucleic Acids Res. 27 (1) (1999) 29–34.
[27] H. Kuwahara, T. Yoshida, Y. Takaki, S. Shimamura, S. Nishi, M. Harada, K. Matsuyama, K. Takishita, M. Kawato, K. Uematsu, Y. Fujiwara, T. Sato, C. Kato, M. Kitagawa, I. Kato, T. Maruyama, Reduced genome of the thioautotrophic intracellular symbiont in a deep-sea clam, *Calyptogena okutanii*, Curr. Biol. 17 (10) (2007) 881–886.
[28] K.J. Livak, T.D. Schmittgen, Analysis of relative gene expression data using real-time quantitative PCR and the 2(T)(-Delta Delta C) method, Methods 25 (4) (2001) 402–408.
[29] D. Fink, Dynamics of Symbiont Abundance in Bathymodiolin Deep-Sea Symbioses 146 Max Plank Institut, Marine Microbiology, Bremen University MPI, Bremen, 2011.
[30] Y. Hongo, T. Ikuta, Y. Takaki, S. Shimamura, S. Shigenobu, T. Maruyama, T. Yoshida, Expression of genes involved in the uptake of inorganic carbon in the gill of a deep-sea vesicomyid clam harboring intracellular thioautotrophic bacteria, Gene 585 (2) (2016) 228–240.
[31] K. Takishita, Y. Takaki, Y. Chikaraishi, T. Ikuta, G. Ozawa, T. Yoshida, N. Ohkouchi, K. Fujikura, Genomic evidence that methanotrophic endosymbionts likely provide deep-sea *Bathymodiolus* mussels with a sterol intermediate in cholesterol biosynthesis, Genome Biol. Evol. 9 (5) (2017) 1148–1160.
[32] T. Ikuta, K. Igawa, A. Tame, T. Kuroiwa, H. Kuroiwa, Y. Aoki, Y. Takaki, Y. Nagai, G. Ozawa, M. Yamamoto, R. Deguchi, K. Fujikura, T. Maruyama, T. Yoshida, Surfing the vegetal pole in a small population: extracellular vertical transmission of an 'intracellular' deep-sea clam symbiont, R. Soc. Open. Sci. 3 (5) (2016).
[33] L.G. Hennighausen, A.E. Sippel, Mouse whey acidic protein is a novel member of the family of 'four-disulfide core' proteins, Nucleic Acids Res. 10 (8) (1982) 2677–2684.
[34] M.S. Kim, M.J. Byun, B.H. Oh, Crystal structure of peptidoglycan recognition protein LB from *Drosophila melanogaster*, Nat. Immunol. 4 (8) (2003) 787–793.
[35] C.P. Swaminathan, P.H. Brown, A. Roychowdhury, Q. Wang, R. Guan, N. Silverman, W.E. Goldman, G.J. Boons, R.A. Mariuzza, Dual strategies for peptidoglycan discrimination by peptidoglycan recognition proteins (PGRPs), Proc. Natl. Acad. Sci. U. S. A 103 (3) (2006) 684–689.
[36] J.H. Lim, M.S. Kim, H.E. Kim, T. Yano, Y. Oshima, K. Aggarwal, W.E. Goldman, N. Silverman, S. Kurata, B.H. Oh, Structural basis for preferential recognition of diaminopimelic acid-type peptidoglycan by a subset of peptidoglycan recognition proteins, J. Biol. Chem. 281 (12) (2006) 8286–8295.
[37] A. Fialamedioni, C. Metivier, A. Herry, M. Lepennec, Ultrastructure of the gill of the hydrothermal-vent mytilid *Bathymodiolus* Sp, Mar. Biol. 92 (1) (1986) 65–72.
[38] L.T. Threadgold, The Ultrastructure of the Animal Cell, 2 ed., (1976) Pergamon.
[39] D. Lo, W. Tynan, J. Dickerson, J. Mendy, H.W. Chang, M. Scharf, D. Byrne, D. Brayden, L. Higgins, C. Evans, D.J. O'Mahony, Peptidoglycan recognition protein expression in mouse Peyer's Patch follicle associated epithelium suggests functional specialization, Cell. Immunol. 224 (1) (2003) 8–16.
[40] R. Bettencourt, M. Rodrigues, I. Barros, T. Cerqueira, C. Freitas, V. Costa, M. Pinheiro, C. Egas, R.S. Santos, Site-related differences in gene expression and bacterial densities in the mussel Bathymodiolus azoricus from the Menez Gwen and Lucky Strike deep-sea hydrothermal vent sites, Fish Shellfish Immunol. 39 (2) (2014) 343–353.
[41] V. Bischoff, C. Vignal, B. Duvic, I.G. Boneca, J.A. Hoffmann, J. Royet, Downregulation of the *Drosophila* immune response by peptidoglycan-recognition proteins SC1 and SC2, PLoS Pathog. 2 (2) (2006) 139–147.
[42] J. Royet, D. Gupta, R. Dziarski, Peptidoglycan recognition proteins: modulators of the microbiome and inflammation, Nat. Rev. Immunol. 11 (12) (2011) 837–851.
[43] J.V. Troll, E.H. Bent, N. Pacquette, A.M. Wier, W.E. Goldman, N. Silverman, M.J. McFall-Ngai, Taming the symbiont for coexistence: a host PGRP neutralizes a bacterial symbiont toxin, Environ. Microbiol. 12 (8) (2010) 2190–2203.
[44] J. Maire, C. Vincent-Monegat, S. Balmand, A. Vallier, M. Herve, F. Masson, N. Parisot, A. Vigneron, C. Anselme, J. Perrin, J. Orlans, I. Rahioui, P. Da Silva, M.O. Fauvarque, D. Mengin-Lecreulx, A. Zaidman-Remy, A. Heddi, Weevil pgrp-lb prevents endosymbiont TCT dissemination and chronic host systemic immune activation, Proc. Natl. Acad. Sci. U. S. A 116 (12) (2019) 5623–5632.
[45] M.S. Goodson, M. Kojadinovic, J.V. Troll, T.E. Scheetz, T.L. Casavant, M.B. Soares, M.J. McFall-Ngai, Identifying components of the NF-kappa B pathway in the beneficial *Euprymna scolopes Vibrio fischeri* light organ symbiosis, Appl. Environ. Microbiol. 71 (11) (2005) 6934–6946.
[46] A. Goto, S. Kurata, The multiple functions of the PGRP family in *Drosophila* immunity, Isj-Invertbr. Surviv J 3 (2) (2006) 103–110.
[47] N. Buchon, N.A. Broderick, B. Lemaitre, Gut homeostasis in a microbial world: insights from *Drosophila melanogaster*, Nat. Rev. Microbiol. 11 (9) (2013) 615–626.
[48] M. Gerdol, M. Gomez-Chiarri, M.G. Castillo, A. Figueras, G. Fiorito, R. Moreira, B. Novoa, A. Pallavicini, G. Ponte, K. Roumbedakis, P. Venier, G.R. Vasta, Immunity in molluscs: recognition and effector mechanisms, with a focus on Bivalvia, in: E. Cooper (Ed.), Advances in Comparative Immunology, Springer, Cham, 2018.
[49] A.E. Douglas, Lessons from studying insect symbioses, Cell Host Microbe 10 (4) (2011) 359–367.
[50] M. Ramet, P. Manfruelli, A. Pearson, B. Mathey-Prevot, R.A.B. Ezekowitz, Functional genomic analysis of phagocytosis and identification of a *Drosophila* receptor for E-coli, Nature 416 (6881) (2002) 644–648.
[51] M. LePennec, M. Diouris, A. Herry, Endocytosis and lysis of bacteria in gill epithelium of *Bathymodiolus thermophilus, Thyasira flexuosa* and *Lucinella divaricata* (bivalve, molluscs), J. Shellfish Res. 7 (3) (1988) 483–489.
[52] W.F. Martin, S. Garg, V. Zimorski, Endosymbiotic theories for eukaryote origin, Philos. Trans. R. Soc. B 370 (1678) (2015).
[53] V.A.R. Huss, Freshwater algal symbioses in protozoa and invertebrates, in: J. Seckbach (Ed.), Enigmatic Microorganisms and Life in Extreme Environments, Springer, Dordrecht, 1999, pp. 641–650.
[54] H. Charles, P. Nardon, Intracellular symbiotic bacteria within insects, in: J. Seckbach (Ed.), Enigmatic Microorganisms and Life in Extreme Environments, Springer, Dordrecht, 1999.
[55] S.K. Davy, D. Allemand, V.M. Weis, Cell biology of cnidarian-dinoflagellate symbiosis, Microbiol. Mol. Biol. Rev. 76 (2) (2012) 229–261.
[56] C. Wentrup, A. Wendeberg, M. Schimak, C. Borowski, N. Dubilier, Forever competent: deep-sea bivalves are colonized by their chemosynthetic symbionts throughout their lifetime, Environ. Microbiol. 16 (12) (2014) 3699–3713.
[57] E. Kadar, R. Bettencourt, V. Costa, R.S. Santos, A. Lobo-Da-Cunha, P. Dando, Experimentally induced endosymbiont loss and re-acquirement in the hydrothermal vent bivalve *Bathymodiolus azoricus*, J. Exp. Mar. Biol. Ecol. 318 (1) (2005) 99–110.